Published in final edited form as:
Cell Calcium. 2009 July ; 46(1): 30–38. doi:10.1016/j.ceca.2009.03.018.

Homeostatic and stimulus-induced coupling of the L-type Ca^{2+} channel to the ryanodine receptor in the hippocampal neuron in slices

Jonathan Berrout[*] and **Masako Isokawa**
Department of Biological Sciences, The University of Texas at Brownsville 80 Fort Brown, Brownsville, TX 78520

Abstract

Activity-dependent increase in cytosolic calcium ($[Ca^{2+}]_i$) is a prerequisite for many neuronal functions. We previously reported a strong direct depolarization, independent of glutamate receptors, effectively caused a release of Ca^{2+} from ryanodine sensitive stores and induced the synthesis of endogenous cannabinoids (eCBs) and eCB-mediated responses. However, the cellular mechanism that initiated the depolarization-induced Ca^{2+} release is not completely understood. In the present study, we optically recorded $[Ca^{2+}]_i$ from CA1 pyramidal neurons in the hippocampal slice and directly monitored miniature Ca^{2+} activities and depolarization-induced Ca^{2+} signals in order to determine the source(s) and properties of $[Ca^{2+}]_i$-dynamics that could lead to a release of Ca^{2+} from the ryanodine receptor. In the absence of depolarizing stimuli, spontaneously-occurring miniature Ca^{2+} events were detected from a group of hippocampal neurons. This miniature Ca^{2+} event persisted in the nominal Ca^{2+}-containing artificial cerebrospinal fluid (ACSF), and increased in frequency in response to the bath-application of caffeine and KCl. In contrast, nimodipine, the antagonist of the L-type Ca^{2+} channel (LTCC), a high concentration of ryanodine, the antagonist of the ryanodine receptor (RyR), and thapsigargin (TG) reduced the occurrence of the miniature Ca^{2+} events. When a brief puff-application of KCl was given locally to the soma of individual neurons in the presence of glutamate receptor antagonists, these neurons generated a transient increase in the $[Ca^{2+}]_i$ in the dendrosomal region. This $[Ca^{2+}]_i$-transient was sensitive to nimodipine, TG, and ryanodine suggesting that the $[Ca^{2+}]_i$-transient was caused primarily by the LTCC-mediated Ca^{2+}-influx and a release of Ca^{2+} from RyR. We observed little contribution from N-or P/Q-type Ca^{2+} channels. The coupling between LTCC and RyR was direct and independent of synaptic activities. Immunohistochemical study revealed a cellular localization of LTCC and RyR in a juxtaposed configuration in the proximal dendrites and soma. We conclude in the hippocampal CA1 neuron that: 1) homeostatic fluctuation of the resting membrane potential may be sufficient to initiate functional coupling between LTCC and RyR, 2) the juxtaposed localization of LTCC and RyR has anatomical advantage of synchronizing a Ca^{2+}-release from RyR upon the opening of LTCC, and 3) the synchronized Ca^{2+}-release from RyR occurs immediately after the activation of LTCC and determines the peak amplitude of depolarization-induced global increase in dendrosomal $[Ca^{2+}]_i$.

Please send correspondence to: Masako Isokawa, Ph.D., Department of Biological Sciences, University of Texas at Brownsville, 80 Fort Brown, Brownsville, TX 78520, 956-882-5731 telephone, 956-882-5043 fax, Email: E-mail: Masako.Isokawa@utb.edu.
[*]Present address: Graduate School of Biomedical Sciences and the Department of Integrative Biology and Pharmacology, The University of Texas Health Science Center at Houston, Houston, TX 77030.

INTRODUCTION

RyR is a representative Ca^{2+} release channel in neurons and expressed densely in the hippocampus (1). RyRs have been reported to be involved in various hippocampal neuron functions including spike afterhyperpolarization (2), gene expression (3), and a release of neurotransmitters and neuropeptides (4 for review). In addition, some forms of synaptic plasticity such as depolarization-induced short-term suppression of excitation (DSE)(5,6) and inhibition (DSI)(7) were reported to involve a release of Ca^{2+} from ryanodine-sensitive stores. In these synaptic responses, a Ca^{2+}-release from RyRs was considered as a source of Ca^{2+} that was necessary to synthesize endogenous cannabinoids (eCB) that mediated these synaptic responses (8,9,10). However, the mechanism involved in the control of $[Ca^{2+}]_i$ in the synthesis of eCB is not completely understood. Little is known about the type of calcium channels that are involved in this process. Thus, we examined the source(s) and the kinetics of $[Ca^{2+}]_i$ that are sensitive to neuronal depolarization and the activation of RyR.

Biophysical properties of hippocampal neurons which could initiate calcium-induced calcium release (CICR) from RyR include action potential generation (11,12,13) and some forms of somatic depolarization (14), although CICR may not be involved in the Ca^{2+} transients evoked by back-propagating action potentials in dendrites (15). Although the NMDA receptor may also trigger a Ca^{2+}-release from RyR (16), the activation of RyR can occur in the presence of the NMDA receptor antagonist (17). Thus, in the present study, we primarily focused on the role of the voltage-gated calcium channels and their functional coupling with RyR.

We measured dendrosomal Ca^{2+} signals taken from a defined population of hippocampal CA1 neurons, and tested our hypothesis of functional coupling between the voltage-gated calcium channels and RyR by directly imaging $[Ca^{2+}]_i$-signals. We used a cell-permeant Ca^{2+} indicator in cultured slice preparations because: 1) some voltage-gated calcium channels such as L-type calcium channel (LTCC) may experience potential rundown when cell-impermeant dyes were introduced by the whole-cell recording configuration, and 2) neurons in cultured hippocampal slices are relatively flat in their anatomical configuration compared with those in acutely prepared slices, and yet contain local synaptic machinery and circuits necessary for synaptic responses, hence optimal for the application of optical imaging techniques.

METHODS

Hippocampal slice culture

Organotypic hippocampal slice culture was prepared as reported previously (17). Sprague-Dawley rat pups (postnatal day 6) were anesthetized with halothane and decapitated. Experimental protocols were approved by the Animal Care and Use Committee of the University of Texas at Brownsville. Brains were removed and the hippocampus was sectioned in 400 μm thick. The slices were cultured at 35°C with 5% CO_2 according to the method of Stoppini (18) for at least a week before they were used for experiments.

Calcium Imaging

For dye-loading, slices were placed on a microscope stage in a Petri dish being bathed with culture media. CA1 pyramidal cell layer was deposited with 0.4 μl of 3.3 mM fluo3-AM in 100%DMSO and 0.05μl of pluronic acid (19). Dye-deposited slices were incubated in 10 μM fluo-3AM for 30–60 min in dark at 35°C. Dye-loaded slices were rinsed and perfused (2ml/min) with oxygenated artificial cerebral spinal fluid (ACSF) consisting of (in mM): 125 NaCl, 25 $NaHCO_3$, 10 Glucose, 2.5 KCl, 1.25 NaH_2PO_4, 2 $CaCl_2$, and 2.5 Mg_2SO_4. For experiments with a nominal concentration of extracellular Ca^{2+}, CaCl was omitted from the ACSF and, in some experiments, 10 mM EGTA was added. Depolarization was induced by a brief local puff

application of KCl (170mM in the puffer micropipette with a tip diameter of 20 μm, 3–10 s ejection using a Picospritzer, General Valve). Caffeine was puff-applied locally (20 mM in the puffer micropipette with a tip diameter of 20 μm, 5–10 s ejection). Ryanodine (10 μM), nimodipine (10 μM), kynurenic Acid (1 mM), ω-agatoxin (250 nM), ω-conotoxin (0.25–1 μM) (all from Sigma), APV (100 μM) and NBQX (10 μM)(both from Tocris), thapsigargin (4 μM, Calbiochem), and tetrodotoxin citrate (1 μM, Alomone Lab) were bath-applied.

Fluorescent signals were collected using water-immersion objectives (Axioscope, Zeiss), a cooled CCD camera (Cascade 128+, Roper Scientific) and a filter wheel (Sutter Instruments), all under the control of imaging software (IPLab, BD Science). Spontaneous miniature Ca^{2+} events were recorded with a 20 ms exposure, and stimulus-evoked $[Ca^{2+}]_i$ signals were recorded with a 50–500 ms exposure. Five to 10 frames were acquired before the stimulus (i.e., a local puff application of KCl or caffeine), and basal fluorescence (F_0) was calculated from these imaging frames. Fifty to 100 frames were acquired after the stimulus. Excitation light was emitted only during the imaging, and one run of imaging was done every 5 min. This imaging paradigm has been confirmed non-harming to the health of our cultured hippocampal neurons in our previous studies that utilized a combined method of $[Ca^{2+}]_i$-imaging and the whole cell patch clamp recording to directly monitor membrane potentials (7,20). $[Ca^{2+}]_i$ signals were quantified as a relative change in the peak fluorescence intensity ($\%\Delta F/F_0$) by selecting a region of interest (ROI)($\Delta F=F_t-F_0$, where F_t is a given image frame). Background was selected from a region away from the cell(s) that were imaged in the same frame, and subtracted from the image of interest. Potential puffing artifacts on $[Ca^{2+}]_i$-signals were assessed as follows. When puffing caused any physical movement or dislocation of imaged neurons, the experiment was discontinued. A control experiment for puffing was obtained by filling a puffer pipette with normal ACSF under which no significant changes occurred in $[Ca^{2+}]_i$-signals.

Immunocytochemistry

Age-matched slice cultures were fixed with 4% paraformaldehyde overnight. After being treated with donkey serum (10%) or BSA (5%) and TritonX-100 (0.2%), the slices were incubated in the combination of CaV1.2 antibody raised in rabbit (1:200, Alomone Lab for LTCC) and RyR antibody raised in goat (1:200, Santa Cruz Biotechnology). Control slices were processed using the same concentration of blocking peptides using the corresponding immunizing protein in each case. Alexa 488 (1:200 anti rabbit) and Alexa 594 (1:200 anti goat) (both from Invitrogen) were used as secondary antibodies for CaV1.2 and RyR, respectively. Slices were mounted on glass slides and viewed with a confocal microscope (Olympus, FluoView300). In order to rule out any potential artifact that may originate in the process of culturing, cryo-sectioned slices (40 μm thick) of the whole brain were prepared from cardially perfused age-matched pups with 4% paraformaldehyde and processed for immunohistochemistry using the identical procedure. We did not find any difference in the pattern of immunofluorescence expression for either RyR or LTCC (CaV1.2) between cultured slices and frozen brain sections.

RESULTS

Miniature $[Ca^{2+}]_i$ events are increased in frequency by caffeine and depolarization

$[Ca^{2+}]_i$-signals were imaged from visualized CA1 pyramidal neurons (Fig. 1A). This method helped us to confirm: 1) Fluo3-AM loaded cells were located in the pyramidal cell layer, and 2) the size and shape of the fluorescing cell soma were in agreement with those of CA1 pyramidal cells. We avoided small sized cells that showed intense fluorescence because these cells were likely astroglia (20).

Fluctuations in basal $[Ca^{2+}]_i$ generated spontaneously-occurring transient $[Ca^{2+}]_i$ peaks. These spontaneous $[Ca^{2+}]_i$ peaks were determined significant when the peak $[Ca^{2+}]_i$-increase was greater than mean ± 2SD (standard deviation) in the $\Delta F/F_0$ (%) value. Significant $[Ca^{2+}]_i$ peaks were defined as miniature $[Ca^{2+}]_i$ events. Frequency of miniature $[Ca^{2+}]_i$ events increased when caffeine was puffed locally on the cell soma for 5 seconds. This increase lasted over 15 min after a single caffeine puff and persisted in the nominal Ca^{2+}-containing ACSF (Fig. 1B). Bath concentration of caffeine, 15 min after a single puff application, was estimated to be 10 μM based on the volume of our imaging chamber and the flow rate of ACSF (2ml/min).

Miniature $[Ca^{2+}]_i$ events were modulated by depolarization (Fig. 1C). When slices were perfused with high K^+ (80 mM)-containing ACSF (the osmolarity was adjusted by reducing NaCl concentration), the frequency of miniature $[Ca^{2+}]_i$ events was increased by 59.3% in average (Fig. 1D), and the amplitude was increased by 26.1% in average (Fig. 1E). These increases were sensitive to thapsigargin (TG, 4 μM bath), ryanodine (10 μM bath) and nimodipine (10 μM bath), and the frequency of miniature $[Ca^{2+}]_i$ events was reduced over 75% (Fig. 1D). Caffeine-induced miniature Ca^{2+} events appeared enhanced in duration in the presence of TTX. The possible enhancement in the duration of caffeine-induced miniature Ca^{2+} events by TTX may reflect a sensitized RyR in the absence of spontaneously-occurring $[Ca^{2+}]_i$ fluctuations and the following binding of agonist (Ca^{2+}) to RyR. On the other hand, TTX inhibited the majority of the miniature Ca^{2+} events generated by KCl. Especially, those of large amplitude were inhibited (Fig. 1C). However, the miniature Ca^{2+} event was not completely blocked by TTX. Those resistant to TTX had a small and short-lasting (quickly decaying) peak. TTX-resistant events occurred as a group, but the frequency of their occurrence was low, and we could not quantify the frequency. We defined our miniature Ca^{2+} events based on the peak amplitude as described above. Thus, it is likely that those miniature Ca^{2+} events consisted of more than one kind of generating mechanism. Legrand et al. (21) reported that the Type 3 RyR (RyR3) showed exclusively voltage-independent spontaneous activity when it was over-expressed in the mouse skeletal muscle. Thus, TTX-resistant Ca^{2+} events in our hippocampal slice culture could originate in RyR3.

Basal $[Ca^{2+}]_i$ fluctuation was stable throughout the experiment in the control ACSF. Background fluorescence did not increase, either. The amplitude of miniature $[Ca^{2+}]_i$ events (measured as $\Delta F/F_0$) remained unchanged and the frequency of miniature $[Ca^{2+}]_i$ events were stable throughout the duration of optical recording up to 2 hours. This suggested that membrane potentials of imaged neurons (although they were not measured directly with electrophysiological methods) did not appear shifted towards either positive or negative, and the cells were maintained healthy throughout the recording. On the other hand, basal $[Ca^{2+}]_i$ fluctuation was decreased below the control level by ryanodine and nimodipine (Fig. 1C). This suggested that RyR-mediated Ca^{2+} release may contribute to determine a basal $[Ca^{2+}]_i$. As described in the Method section, excitation light was emitted only during the imaging (50 msec of exposure time for 100 frames per trial, one trial every 5 min). This substantially contributed to avoid any phototoxicity or excitotoxicity.

In summary, the present finding suggests that some RyRs must be constitutively active at a random frequency in a given neuron within the range of homeostatic fluctuation in the membrane potential, and RyR-mediated Ca^{2+} release could occur independent of action potential generation in the CA1 pyramidal neuron. Our data also suggest that depolarization increases the frequency of RyR opening as indicated by the increase in the miniature Ca^{2+} events, and LTCC appears to be involved in the depolarization-induced Ca^{2+}-release from RyRs in the somatodendritic compartment of CA1 hippocampal pyramidal cells.

Macroscopic Ca^{2+} signals mediated by caffeine and KCl

CA1 pyramidal neurons in cultured hippocampal slices showed dense and discrete RyR immunoreactivity in the proximal dendrites, soma, and the nucleus (Fig. 2A). This expression pattern was similar to that of cardially-perfused whole brain of age-matched rat pups (our personal observation) suggesting that slice culture method successfully preserved the physiological pattern of RyR expression. A brief local puff application of caffeine from a micropipette, which was positioned immediately above the cells imaged, induced a global $[Ca^{2+}]_i$-increase in a group of neurons (Fig. 2B). The onset of this $[Ca^{2+}]_i$-increase was phase-locked to the application of caffeine. On the other hand, the duration of this $[Ca^{2+}]_i$-increase outlasted the duration of caffeine-puff suggesting the probable occurrence of a large scale CICR as shown in the average trace of caffeine-responses taken from a group of neurons (Fig. 2C1 arrow). Indeed, a single recording of caffeine-induced $[Ca^{2+}]_i$-signal (in response to a single caffeine-puff of 1.5s), taken from a single neuron, exhibited many small Ca^{2+} peaks during the decay period following the initial $[Ca^{2+}]_i$-peak (inset in Fig. 2C1) suggesting a multiple occurrence of local CICR within a given neuron. However, when $CaCl_2$ was omitted from ACSF (0$[Ca^{2+}]_o$), caffeine-induced $[Ca^{2+}]_i$-increase was restricted within the duration of caffeine-puff and produced only an initial $[Ca^{2+}]_i$ spike suggesting the limited occurrence of CICR (Fig. 2D inset)(also see 22).

Repeated application of caffeine puffs (eight puffs, 5s-long each, an inter-puff interval of 50s) depleted internal Ca^{2+} stores as demonstrated by the loss of Ca^{2+} peaks (Fig. 2C2 and C3). Depletion of stored Ca^{2+} also occurred in the absence of extracellular Ca^{2+} when caffeine was puffed repeatedly onto the identical population of neurons every 10 min (Fig. 2D). The pattern of depletion was similar to those shown in C2 and C3 of Figure 2 (which were acquired in normal Ca^{2+}-containing ACSF) and exhibited two types of release properties as shown in Cell 1 and Cell 2 in Fig. 2D.

We tested if depolarization caused a release of Ca^{2+} from RyRs in the absence of extracellular Ca^{2+}. Hippocampal slices were incubated in the ACSF that contained 2.5 mM of Ca^{2+}. The CA1 pyramidal cells were depolarized by a brief local application of KCl from a micropipette (170 mM in pipette for 10 s). An increase in $[Ca^{2+}]_i$ was detected as a relative increase of fluorescence in 80–140% in $\Delta F/F_0$ (Fig. 2E). After acquiring three consecutive $[Ca^{2+}]_i$-measurements in every 5 min, the extracellular solution was replaced with nominal Ca^{2+}-containing ACSF (specified as 0$[Ca^{2+}]$o in Fig. 2E). Five consecutive application of KCl puffs (10 sec puff in every 5 min) generated $[Ca^{2+}]_i$-increases in nominal Ca^{2+}-containing ACSF with the magnitude similar to those evoked in the Ca^{2+}-containing ACSF (arrows in Fig. 2E). These results were in agreement with those obtained in nominal Ca^{2+}-containing ACSF that also contained 10 mM EGTA (data not shown). This finding suggested that a Ca^{2+}-release from RyRs may occur in response to depolarization in the absence of extracellular Ca^{2+}. Indeed, a subtype of RyR has been reported to generate a spontaneous release of Ca^{2+} in response to membrane voltage, independent of Ca^{2+} in the hypothalamic neurons (23). As reported previously (1), hippocampal neurons express all three RyR subtypes. Thus, a Ca^{2+}-independent release of Ca^{2+} from RyRs may exist in the hippocampal neurons as a homeostatic mechanism to regulate $[Ca^{2+}]_i$ in response to constantly-changing membrane potentials. It needs to be determined whether a Ca^{2+}-independent release of Ca^{2+} in response to depolarization and the TTX-insensitive miniature Ca^{2+} events share the same release mechanism under the unified RyR subtypes.

Juxtaposed expression of somal LTCC (CaV1.2) and RyR

Hippocampal CA1 neurons in our cultured slice preparations exhibited dense immunoreactivity to the L-type calcium channel (LTCC) when we used an antibody against CaV1.2 with a fluorochrome-conjugated secondary antibody (Alexa 488).

Immunofluorescence was densest in the stratum radiatum where proximal apical dendrites of the CA1 pyramidal neuron are located (Fig. 3A2). Pyramidal cell soma was also strongly immunoreactive. Dual labeling of CaV1.2 with RyR (Alexa 594) revealed a juxtaposed pattern of concentric expression between LTCC and RyR in the somata and proximal dendrites of CA1 pyramidal neurons (Fig. 3A3 and A4). RyR immuno-reactivity exhibited local hot spots suggesting that RyRs were expressed in a discrete manner in the cytoplasm, in particular, on the membrane of the endoplasmic reticulum (ER) that extended closely to the plasma membrane as well as on the nucleus (Fig. 3B3 and Fig. 2A). The probability of RyR extending to the proximity of LTCC appeared substantial in our preparations as demonstrated by the intense labeling of these two channels being juxtaposed each other (Fig. 3C1, C2, and C3). It is helpful to mention about our filter system between laser channels, as well as un-likeliness of cross excitation and bleed-through emission between the secondary antibodies that we used (Alexa 488 and Alexa 594). Spectra for Alexa 488 (blue excitation) and Alexa 594 (yellow excitation) are well separated. The wavelength of 488 excites a fluorochrome of only green-emission without any cross excitation of a fluorochrome whose excitation wavelength is 594, although 488 could excite a fluorochrome whose excitation wavelength is 561. A dichroic filter of 565 also helped us to separate the excitation of these two fluorochromes (Alexa 488 and 594). Emission bleed-through was prevented by using a band-pass emission filter that allowed us to collect longer wavelengths. In conclusion, our immunofluorescence data provide anatomical evidence for the physical proximity of these two Ca^{2+} permeable channels and support our Ca^{2+} imaging data that suggest the occurrence of functional coupling between RyR and LTCC in the dendrosomal regions of the CA1 pyramidal neuron.

Depolarization-induced $[Ca^{2+}]_i$–signals are sensitive to antagonists of LTCC and RyR

A brief local puff application of KCl from a micropipette onto visually-identified CA1 pyramidal neurons evoked a transient $[Ca^{2+}]_i$-elevation (Fig. 4A). The duration of this $[Ca^{2+}]_i$-elevation equaled to the duration of KCl application. In some neurons, however, the $[Ca^{2+}]_i$-elevation outlasted the duration of KCl application for several tens of seconds, suggesting that KCl might have caused a polysynaptic increase of $[Ca^{2+}]_i$. These responses were excluded from further analysis.

$[Ca^{2+}]_i$-elevation, evoked by the brief local KCl-puff, was sensitive to ryanodine (10 μM), and the amplitude of $[Ca^{2+}]_i$-peak was reduced by 49% in average (n= 21)(Fig. 4A). The magnitude of reduction was independent of synaptically-induced depolarization because it was not affected by kynurenic acid or the combined application of APV (100 μM) and NBQX (10 μM)(n=15, Fig 4B1, data were pooled in this figure). However, the peak amplitude of $[Ca^{2+}]_i$ ($\%\Delta F/F_0$) in the presence of kynurenic acid (or the combination of APV and NBQX) was smaller and less than 50% of the original $[Ca^{2+}]_i$-peak in the absence of these antagonists. This suggested that: 1) KCl-induced depolarization caused a release of glutamate and activated the receptor-mediated Ca^{2+}-permeable channels synaptically, 2) the glutamate receptor-dependent $[Ca^{2+}]_i$-increase could constitute up to 50% of the total $[Ca^{2+}]_i$-elevation induced by KCl; however, 3) the ratio of reduction by ryanodine in the KCl-induced $[Ca^{2+}]_i$-elevation was not affected by the blockade of ionotropic glutamate receptors, suggesting little contribution of the Ca^{2+}-permeable glutamate receptor channels under the current depolarization protocol.

$[Ca^{2+}]_i$-elevation, evoked by a local puff-application of caffeine, was blocked when slices were pre-incubated in thapsigargin (TG, 4 μM in the bath ACSF)(Fig. 4B2). $[Ca^{2+}]_i$-elevation, evoked by a brief local KCl-puff, was also sensitive to TG. The amplitude of $[Ca^{2+}]_i$-peak was reduced by 69% in average (n= 14)(Fig. 4B3). Interestingly, when caffeine was puff-applied immediately before the puff-application of KCl, $[Ca^{2+}]_i$-peak was enhanced in the control ACSF (Fig. 4B3). These data supported our interpretation that depolarization-induced

$[Ca^{2+}]_i$-increase did indeed involved the activation of RyR and the subsequent release of Ca^{2+} from internal stores.

We tested N- and P/Q-type calcium channel inhibitors for their possible coupling with RyR. In the presence of APV (100 μM) and NBQX (10 μM), or with kynurenic acid (1 mM), the N-type channel inhibitor, ω-conotoxin (0.25–1 μM) did not have any effect on the KCl-induced $[Ca^{2+}]_i$-increase. In the presence of ω-conotoxin, the amplitude of KCl-induced $[Ca^{2+}]_i$ peak remained unchanged (n=7, Fig. 4C2). On the other hand, the P/Q-type channel inhibitor, ω-agatoxin (250 nM) had minimal but significant effect on the KCl-induced $[Ca^{2+}]_i$-increase. With ω-agatoxin (250 nM) in the bath, the amplitude of KCl-induced $[Ca^{2+}]_i$-peak was attenuated (n=6, Fig. 4C3, $p<0.01$). This reduction might have reflected the presence of P/Q type calcium channels in the distal dendrites of our CA1 hippocampal neurons (24) possibly contributing to depolarization-induced somal $[Ca^{2+}]_i$ signaling.

In a separate group of neurons (n=10), the effect of nimodipine (10 μM) was tested. Nimodipine became effective quickly, and decreased the peak amplitude within 5 min of its application (Fig. 4D). Nimodipine decreased the amplitude of KCl-induced $[Ca^{2+}]_i$-peak by 82% of the original in the presence of kynurenic acid (Fig. 4B1). This reduction was similar in the magnitude to the reduction caused by nimodipine in the absence of the ionotropic glutamate receptor antagonists (Fig. 4C1), suggesting that LTCC is a major source of depolarization-induced $[Ca^{2+}]_i$-elevation independently of the ionotropic glutamate receptors.

The amplitude of KCl-induced $[Ca^{2+}]_i$-peak was reduced to 1/5 of the original by nimodipine, and further reduced to 1/10 of the original by the combined application of nimodipine and ryanodine. Although the reduction in the amplitude of KCl-induced $[Ca^{2+}]_i$-peak caused by ryanodine was smaller in the presence of nimodipine, the reduction was significant ($p<0.001$) (Fig. 4E1 for group data, n=10). However, neither nimodipine nor ryanodine shortened the duration of $[Ca^{2+}]_i$-signals induced by depolarization caused by KCl. KCl-induced $[Ca^{2+}]_I$-peak in the presence of kynurenic acid was also sensitive to nimodipine and ryanodine (Fig. 4E2). Ryanodine reduced the peak amplitude by 45.4% in average in the presence of kynurenic acid. This suggested that the kynurenic acid-sensitive $[Ca^{2+}]_i$-signal was less sensitive to ryanodine than the nimodipine-sensitive $[Ca^{2+}]_i$-signal.

DISCUSSION

We demonstrated in the hippocampal CA1 pyramidal cell in slice preparations that: 1) a Ca^{2+} release occurred spontaneously from RyR at a resting level of membrane potential, 2) LTCC was a major source to prime a depolarization-induced Ca^{2+} release from RyR, and 3) RyR-mediated Ca^{2+} release determined the kinetics and peak amplitude of depolarization-induced somatodendritic $[Ca^{2+}]_i$-signals. The present study also demonstrated that a brief local puff-application of KCl from a micropipette, visually positioned just above the soma of a Ca^{2+} indicator-loaded hippocampal pyramidal cell, could provide sufficient spatial and temporal resolutions for the measurement of dendrosomal $[Ca^{2+}]_i$-signals mediated by LTCC and RyR.

The involvement of RyR in the depolarization-induced Ca^{2+}-release has been reported in several different types of neurons including cerebellar granule cells (2), hippocampal CA3 neurons (25), and sympathetic neurons (26). These studies showed the role of RyR in the activation of the Ca^{2+}-mediated K^+ channel with or without the involvement of other neurotransmitter receptors using electrophysiological and pharmacological techniques. They did not provide detailed information on the $[Ca^{2+}]_i$ kinetics that were mediated by RyR. In the dorsal root ganglion neurons (27), $[Ca^{2+}]_i$ kinetics were studied in the depolarization-induced release of Ca^{2+} from RyR; however, no significant coupling was detected between LTCC and

RyR. In the hippocampus, there are studies that reported $[Ca^{2+}]_i$ dynamics induced by depolarization that involved the activation of RyR (11–16). However, none of these studies identified the L-type Ca^{2+} channel as the primary plasma membrane Ca^{2+} channel that can directly activate RyR. Our paper is the first to demonstrate, by directly monitoring $[Ca^{2+}]_i$ kinetics in individual hippocampal neurons, that a Ca^{2+} release from internal stores is recruited to maintain homeostatic (basal) $[Ca^{2+}]_i$ activity as well as during neuronal depolarization through a direct functional coupling with the L-type Ca^{2+} channel.

Concentration of cytosolic calcium ($[Ca^{2+}]_i$) has been reported to fluctuate in response to constantly-changing synaptic environment. Even in the absence of external input, hippocampal pyramidal neurons are spontaneously active, and this ongoing homeostatic activity could be detected by calcium imaging. We found that caffeine and high concentration of extracellular K^+ increased the frequency of spontaneously occurring miniature $[Ca^{2+}]_i$-events. These miniature events were sensitive to nimodipine, TG, and a micromole concentration of ryanodine. These findings suggest that spontaneously occurring miniature $[Ca^{2+}]_i$-events may likely represent spontaneously occurring Ca^{2+} releases from RyRs, and a Ca^{2+} releases from RyR could occur constitutively under the physiological range of fluctuations in the membrane potential. The constitutive release of Ca^{2+} from RyR may contribute to a constitutive synthesis and release of an endogenous cannabinoid in the hippocampal neuron. Indeed, this possibility is supported by the report on the constitutive activation of the cannabinoid receptor (CB1R) in the hippocampal neuron (28).

When $[Ca^{2+}]_i$-increase was evoked by depolarization (i.e., a brief local puff application of KCl), the duration of evoked $[Ca^{2+}]_i$-response lasted as long as the depolarization lasted. The time to peak (τ) in the evoked $[Ca^{2+}]_i$-increase was a function of the duration of depolarization. In the present study, ryanodine and thapsigargin retarded the rate of rise and peak amplitude of LTCC-initiated $[Ca^{2+}]_i$-increase without changing the time constant (τ) to peak. From this observation, it was evident that RyR-mediated CICR occurred at the moment when LTCC was activated. RyRs have fast activation time constants, ranging from 0.5 to 1 ms, regardless of the type of RyR isoform (29). Hippocampal neurons express all three isoforms (1). Thus, prominent RyR-mediated responses are not unexpected in the hippocampus. In addition, we should mention the possible involvement of the ADP-ribosyl cyclase in the functional coupling of RyR with the L type Ca channels in neurons (30). One of the functions of ADP-ribosyl cyclase is to synthesize cADP ribose, which stimulates the function of RyR. ADP-ribosyl cyclase translocates from the cytosol into the nucleus upon depolarization, and this translocation appears dependent on a calcium influx mediated by the L-type calcium channel. Thus, the ADP-ribosyl cyclase could be a molecule that is involved to initiate the functional coupling between the ryanodine receptor and LTCC in the hippocampal neurons.

Our immunocytochemical findings demonstrated the proximity of LTCC and RyR, and showed that they were arranged in a concentric manner around the plasma membrane in the soma. The close apposition to the cell membrane of subsurface cisterns and the extensions of RyR-bearing ER (31,32) may provide morphological substrate to our findings and support our interpretation for the existence of anatomical and functional coupling between LTCC and RyR. We propose a critical interpretation, by demonstrating the cellular distribution of RyR in the hippocampal neurons, that the RyR-expressing ER membrane extends close to the plasma membrane forming a donut-like configuration while accommodating a large nucleus. Strong RyR expression close to the plasma membrane provides structural evidence for functional coupling between RyR and LTCC even if physical closeness may not be sufficient by itself to provide direct evidence for functional communication.

The involvement of voltage-gated Ca^{2+} channels was previously suggested in several forms of retrograde signaling mediated by molecules. However, no discussion was raised in these

studies for the involvement of store-released Ca^{2+} (33,34). Our present findings provide direct experimental evidence to much-argued relationships between voltage-gated calcium channels and calcium release channels in the hippocampal neuron, and suggest their contribution to hippocampal neuron functions that involve endogenous cannabinoids as a retrograde messenger.

Finally, the possibility of Ca^{2+}-independent activation of neuronal RyR by LTCC should be mentioned. Recent studies in the hypothalamic neuron axon terminals (23) and ventricular myocytes in the heart (35) showed a localized elementary Ca^{2+} release from RyR, which occurred independently of Ca^{2+} entry and was sensitive to dihydropyridine receptor antagonists. These Ca^{2+} release persisted in the absence of extracellular Ca^{2+}, and increased their frequency in response to depolarization. In the present study, we showed evidence that supports a voltage-dependent and Ca^{2+} independent release of Ca^{2+} (Fig. 2E). Our $[Ca^{2+}]_i$ signals of evoked and miniature events were sensitive to nimodipine, which directly blocks LTCC channel pores and prevents Ca^{2+} influxes. However, the hippocampal neurons express all three subtypes of RyRs. This complexity may make an interpretation difficult. Even if Ca^{2+}-independent activation had occurred through RyR1 (as is the case in the hypothalamic neuron) or RyR3 (as is the case in the skeletal muscle) in tandem with the activation of LTCC in the present study, it might have been masked by simultaneous activation of the remaining subtypes of RyRs. Genetic manipulation of subtype-specific RyR expression in the cultured hippocampus might be required to dissect a potential Ca^{2+}-independent form of RyR activation and to determine whether such activation provides a molecular mechanism for Ca^{2+}-signals that can contribute to hippocampal synaptic plasticity.

Acknowledgments

This work was supported by a NIH grant R15DA021683 and SC1GM081179 (to M.I.). J. Berrout is a recipient of a Student Travel Award from the Faculty in Undergraduate Neuroscience in 2006.

References

1. Sharp AH, McPherson PS, Dawson TM, Aoki C, Campbell KP, Snyder SH. Differential immunohistochemical localization of inositol 1,4,5-trisphosphate- and ryanodine-sensitive Ca^{2+} release channels in rat brain. J Neurosci 1993;13:3051–3063. [PubMed: 8392539]
2. Chavis P, Fagni L, Lansman JB, Bockaert J. Functional coupling between ryanodine receptors and L-type calcium channels in neurons. Nature 1996;382:719–722. [PubMed: 8751443]
3. Bito H, Deisseroth K, Tsien RW. CREB phosphorylation and dephosphorylation: a Ca and stimulus duration-dependent switch for hippocampal gene expression. Cell 1996;87:1203–1214. [PubMed: 8980227]
4. Bouchard R, Pattarini R, Geiger JD. Presence and functional significance of presynaptic ryanodine receptors. Prog Neurobiol 2003;69:391–418. [PubMed: 12880633]
5. Melis M, Perra S, Muntoni AL, Pillolla G, Lutz B, Marsicano G, Di Marzo V, Gessa GL, Pistis M. Prefrontal cortex stimulation induces 2-arachidonoylglycerol-mediated suppression of excitation in dopamine neurons. J Neurosci 2004;24:10707–10715. [PubMed: 15564588]
6. Straiker A, Mackie K. Depolarization-induced suppression of excitation in murine autaptic hippocampal neurons. J Physiol 2005;569:501–517. [PubMed: 16179366]
7. Isokawa M, Alger BE. Retrograde endocannabinoid regulation of GABAergic inhibition in the dentate gyrus granule cell. J Physiol 2005;567:1001–1010. [PubMed: 16037085](On-line publication on July 25, 2005)
8. Wilson RI, Nicoll RA. Endogenous cannabinoids mediate retrograde signaling at hippocampal synapses. Nature 2001;410:588–595. [PubMed: 11279497]
9. Ohno-Shosaku T, Maejima T, Kano M. Endogenous cannabinoids mediate retrograde signals from depolarized postsynaptic neurons to presynaptic terminals. Neuron 2001;29:729–738. [PubMed: 11301031]

10. Cadas H, Gaillet S, Beltramo M, Vanance L, Piomelli D. Biosynthesis of an endogenous cannabinoid precursor in neurons and its control by calcium and cAMP. J Neurosci 1996;16:3934–3942. [PubMed: 8656287]
11. Jacobs JM, Meyer T. Control of action potential-induced Ca2_ signaling in the soma of hippocampal neurons by Ca2_ release from intracellular stores. Neuroscience 1997;17:4129–4135. [PubMed: 9151730]
12. Sandler VM, Barbara JG. Calcium-induced calcium release contributes to action potential-evoked calcium transients in hippocampal CA1 pyramidal neurons. Neuroscience 1999;19:4325–4336. [PubMed: 10341236]
13. Sabatini BL, Oertner TG, Svoboda K. The life cycle of Ca ions in dendritic spines. Neuron 2002;33:439–452. [PubMed: 11832230]
14. Garaschuk O, Yaari Y, Konnerth A. Release and sequestration of calcium by ryanodine-sensitive stores in rat hippocampal neurones. J Physiol 1997;502:13–30. [PubMed: 9234194]
15. Markram H, Helm PJ, Sakmann B. Dendritic calcium transients evoked by single back-propagating action potentials in rat neocortical pyramidal neurons. J Physiol 1995;485:1–20. [PubMed: 7658365]
16. Moriguchi S, Nishi M, Komazaki S, Sakagami H, Miyazaki T, Masumiya H, Saito SY, Watanabe M, Kondo H, Yawo H, Fukunaga K, Takeshima H. Functional uncoupling between calcium release and afterhyperpolarization in mutant hippocampal neurons lacking junctophilins. Proc Nagl Acad Sci USA 2006;103:10811–10816.
17. Isokawa M, Alger BE. The ryanodine receptor regulates endogenous cannabinoid mobilization in the hippocampus. J Neurophysiol 2006;95:3001–11. [PubMed: 16467427](Epub 2006 Feb 8.)
18. Stoppini L, Buchs PA, Muller D. A simple method for organotypic cultures of nervous tissue. J Neurosci Methods 1991;37:173–182. [PubMed: 1715499]
19. MacLean JN, Fenstermaker V, Watson BO, Yuste R. A visual thalamocortical slice. Nat Methods 2006;3:129–134. [PubMed: 16432523]
20. Sasaki T, Matsuki N, Ikegaya Y. Metastability of Active CA3 Networks. J Neurosci 2007;27:517–528. [PubMed: 17234584]
21. Legrand C, Giacomello E, Berthier C, Allard B, Sorrentino V, Jacquemond V. Spontaneous and voltage-activated Ca^{2+} release in adult mouse skeletal muscle fibers expressing the type 3 ryanodine receptor. J Physiol 2008;586:441–457. [PubMed: 18006577]
22. Friel DD, Tsien RW. A caffeine-and ryanodine-sensitive Ca^{2+} store in bullfrog sympathetic neurons modulates effects of Ca^{2+} entry on $[Ca^{2+}]i$. J Physiol 1992;450:217–246. [PubMed: 1432708]
23. De Crescenzo V, ZhuGe R, Velazquez-Marrero V, Lifshitz LM, Custer E, Carmichael J, Lai TA, Tuft RA, Fogarty KE, Lemos JR, Walsh JV Jr. Ca^{2+} syntillas, miniature Ca^{2+} release events in terminals of hypothalamic neurons, are increased in frequency by depolarization in the absence of Ca^{2+} influx. J Neurosci 2004;24:1226–1235. [PubMed: 14762141]
24. Kavalali ET, Zhuo M, Bito H, Tsien RW. Dendritic Ca2+ channels characterized by recordings from isolated hippocampal dendritic segments. Neuron 1997;18:651–63. [PubMed: 9136773]
25. Swartz KJ, Bean BP. Inhibition of Ca2+ channels in rat CA3 pyramidal neurons by a metabotropic glutamate receptor. J Neurosci 1992;12:4358–4371. [PubMed: 1359036]
26. Akita T, Kuba K. Functional triads consisting of ryanodine receptors, Ca2+ channels, and Ca2+-activated K+ channels in bullfrog sympathetic neurons. Plastic modulation of action potential. J Gen Physiol 2000;116:697–720. [PubMed: 11055998]
27. Usachev YM, Thayer SA. All-or-None Ca^{2+} Release from Intracellular Stores Triggered by Ca^{2+} Influx through Voltage-Gated Ca^{2+} Channels in Rat Sensory Neurons. J Neurosci 1997;17:7404–7414. [PubMed: 9295386]
28. Losonczy A, Biro AA, Nusser Z. Persistently active cannabinoid receptors mute a subpopulation of hippocampal interneurons. Proc Natl Acad Sci U S A 2004;101:1362–1367. [PubMed: 14734812]
29. Fill M, Copello JA. Ryanodine receptor calcium release channels. Physiol Rev 2002;82:893–922. [PubMed: 12270947]
30. Bezin S, Charpentier G, Lee HC, Baux G, Fossier P, Cancela JM. Regulation of nuclear Ca^{2+} signaling by translocation of the Ca^{2+} messenger synthesizing enzyme ADP-ribosyl cyclase during neuronal depolarization. J Biol Chem 2008;283:27859–27870. [PubMed: 18632662]

31. Benedeczky I, Molnar E, Somogyi P. The cisternal organelle as a Ca2+-storing compartment associated with GABAergic synapses in the axon initial segment of hippocampal pyramidal neurones. Exp Brain Res 1994;101:216–230. [PubMed: 7843310]

32. Berridge MJ. Neuronal calcium signaling. Neuron 1998;21:13–26. [PubMed: 9697848]

33. Jo YH, Chen Y-JJ, Chua SC Jr, Talmage DA, Role LW. Integration of endocannabinoid and leptin signaling in an appetite-related neural circuit. Neuron 2005;48:1055–1066. [PubMed: 16364907]

34. Bolshakov VY, Siegelbaum SA. Hippocampal long-term depression: arachidonic acid as a potential retrograde messenger. Neuropharmacology 1995;34:1581–1587. [PubMed: 8606806]

35. Copello JA, Zima AV, Diaz-Sylvester PL, Fill M, Blatter LA. Ca^{2+} entry-independent effects of L-type Ca^{2+} channel modulators on Ca^{2+} sparks in ventricular myocytes. Am J Physiol Cell Physiol 2007;292:C2129–2140. [PubMed: 17314267]Epub 2007 Feb 21

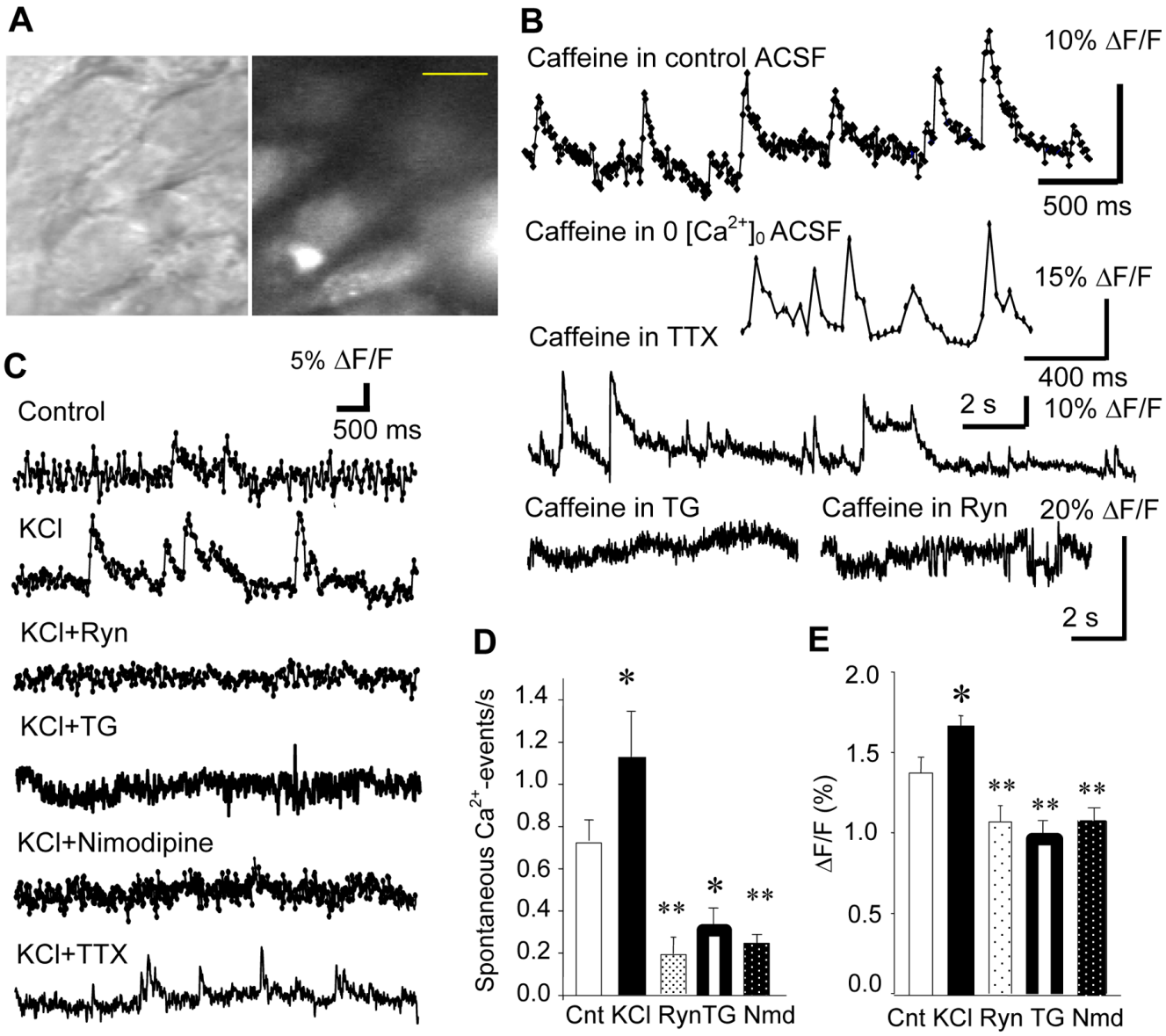

Figure 1.

Miniature $[Ca^{2+}]_i$ events in the CA1 pyramidal cell. **A**. Visually-identified CA1 pyramidal cells with DIC (left) were loaded with fluo-3AM (right). Calibration bar: 10 μm. **B**. Caffeine enhanced the probability of generating miniature $[Ca^{2+}]_i$-events, which persisted in the Ca^{2+}-free ACSF and in the tetrodotoxin (TTX, 1 μM)-containing ACSF. However, caffeine was not effective of generating any $[Ca^{2+}]_i$-event in the presence of thapsigargin (TG, 4 μM) and ryanodine (Ryn, 10 μM). **C**. Miniature $[Ca^{2+}]_i$-events in the control ACSF, 80 mM K^+-containing ACSF, 80 mM K^+ and ryanodine-containing ACSF, 80 mM K^+ and TG-containing ACSF, 80 mM K^+ and nimodipine-containing ACSF, and 80 mM K^+ and TTX-containing ACSF. **D**. Mean frequency of miniature $[Ca^{2+}]_i$-events in the above 5 experimental conditions (excluding TTX experiment, see text for explanations). **E**. Mean amplitude (measured as % $\Delta F/F_0$) of miniature $[Ca^{2+}]_i$ events in the 5 conditions. Cnt: Control, KCl: 80mM K^+-containing ACSF, Ryn: ryanodine and 80 mM K^+-containing ACSF, TG: thapsigargin and 80 mM K^+-containing ACSF, Nmd: nimodipine and 80 mM K^+-containing ACSF.

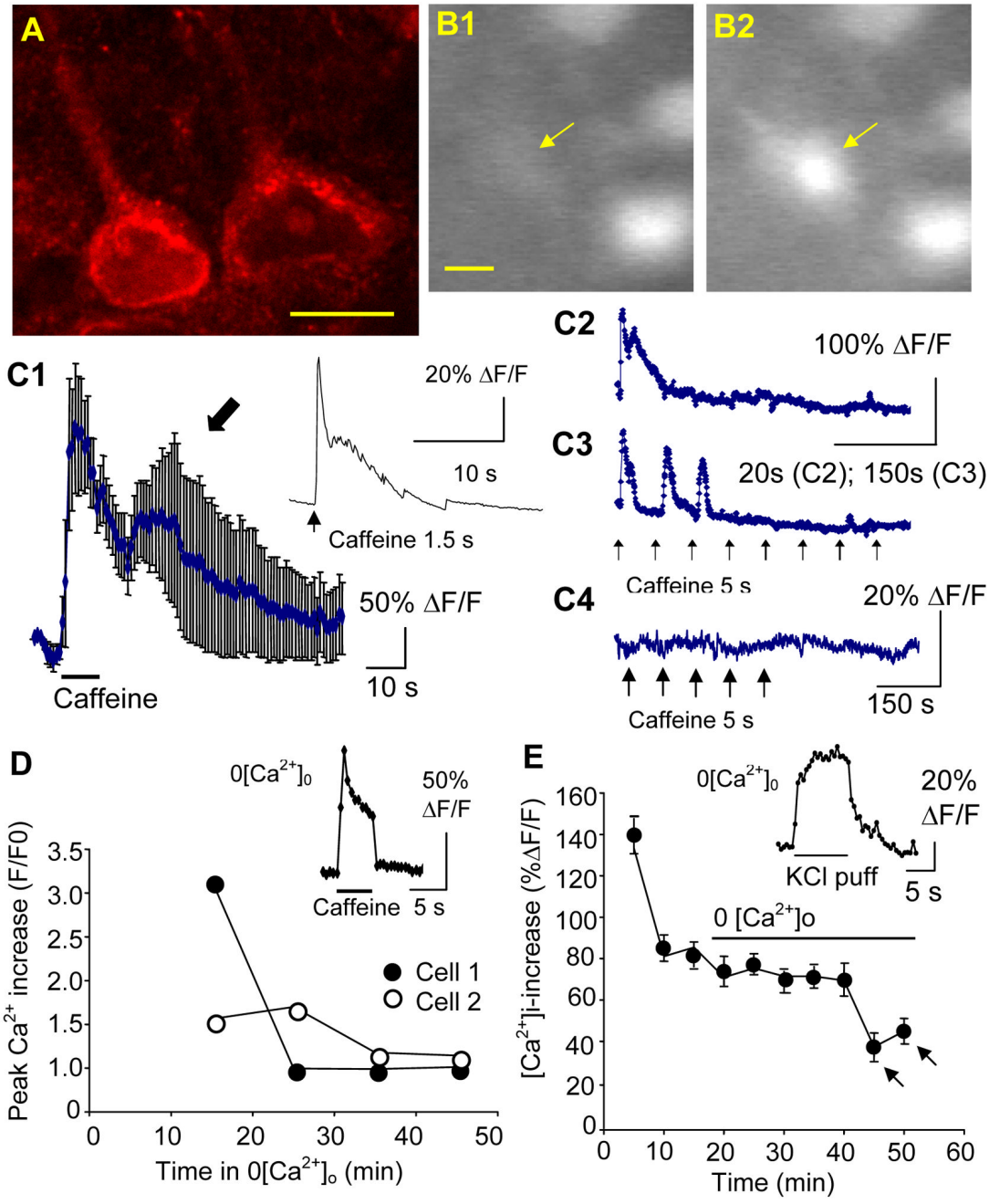

Figure 2.

Cellular expression of RyR and caffeine-induced $[Ca^{2+}]_i$-responses. **A**. A confocal image of RyR immunoreactivity in the CA1 pyramidal cell. **B**. Fluo-3AM-loaded pyramidal cells increased $[Ca^{2+}]$i-signals in response to a puff-application of caffeine (B1: before, B2: after). Calibration bar: 10 μm in A and B. **C**. Caffeine-induced $[Ca^{2+}]_i$-increase in control ACSF (C1:Mean ± SEM in 5 cells). Inset in C1 shows a single caffeine response in single neuron. Repeated caffeine puffs (5s-puff, indicated by black arrows) depleted caffeine-sensitive Ca^{2+} stores (two representative patterns of depletion in C2 and C3). Caffeine puffs were not effective of generating any $[Ca^{2+}]_i$-increase in the presence of thapsigargin (TG: 4 μM, C4). **D**. Time-dependent changes in the caffeine-induced $[Ca^{2+}]_i$-response in $0[Ca^{2+}]_o$ ACSF in two

neurons, each with a representative release property. Inset shows a Ca^{2+} response to a single caffeine puff in a single neuron in 0$[Ca^{2+}]_o$ ACSF. **E**. KCl-induced $[Ca^{2+}]_i$-increase in 0 $[Ca^{2+}]_o$ ACSF. The plot shows the average and SEM of peak $[Ca^{2+}]_i$-increase caused by KCl in 7 neurons. Inset shows a $[Ca^{2+}$]i-increase in response to a single KCl application in a single neuron in 0$[Ca^{2+}]_o$ ACSF.

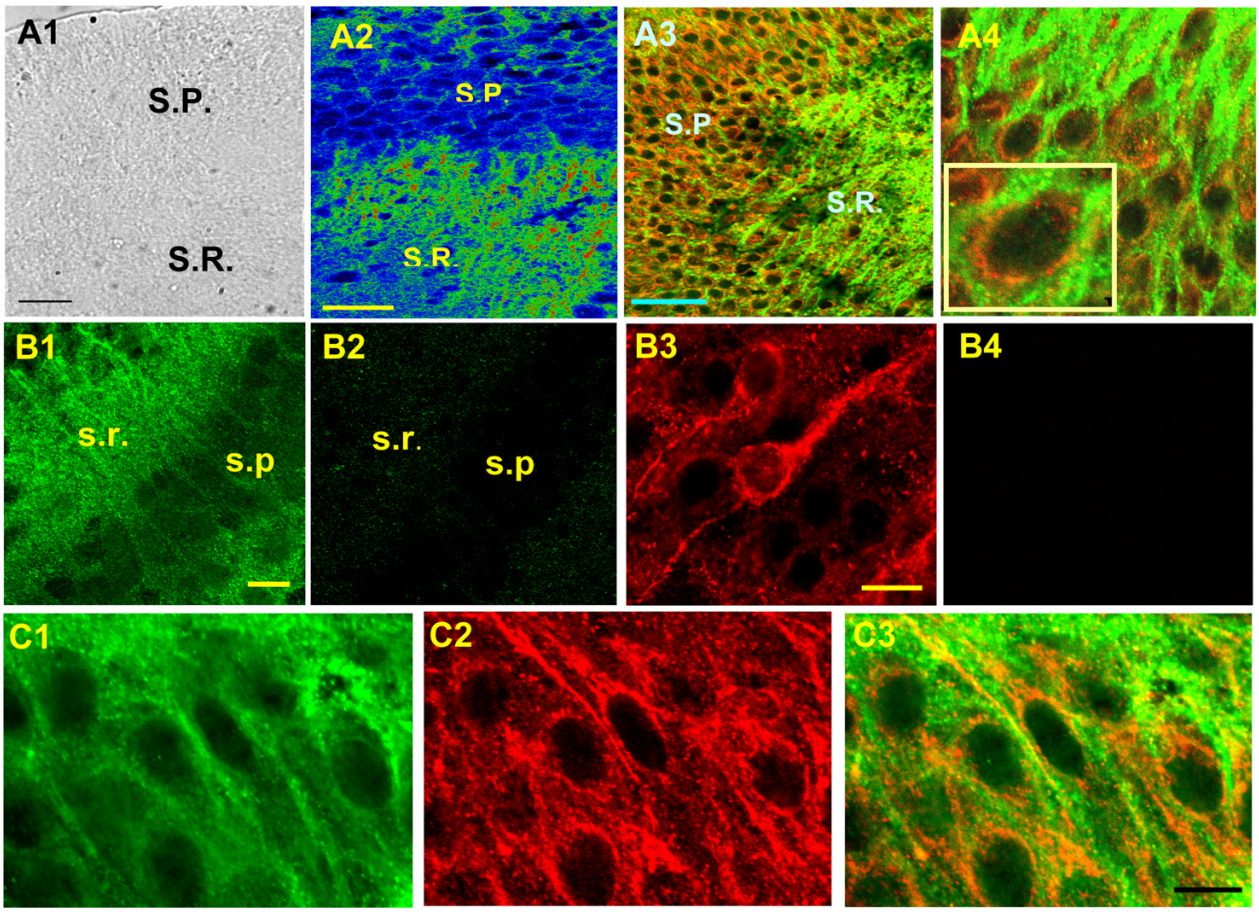

Figure 3.

Juxtaposed localization of RyR and LTCC (CaV1.2). **A1**. A bright field image of the hippocampal slice culture that was used for dual labeling of RyR and CaV1.2. **A2**. CaV1.2 immunoreactivity in CA1 (warmer color represents stronger immunoreactivity). **A3**. Dual labeling of RyR (red) and CaV1.2 (green). SP: Stratum Pyramidale, SR: Stratum Radiatum. **A4**. Dual labeling in the pyramidal cell layer with higher magnification. **B1**. CaV1.2. **B2**. CaV1.2 with a blocking peptide. **B3**. RyR, **B4**. RyR with a blocking peptide. **C1**–**3**. Dual labeling of CaV1.2 and RyR with an image of CaV1.2 only (C1), RyR only (C2), and a merged image of both CaV1.3 and RyR (C3). These three images were taken sequentially from the identical population of the neurons in the same slice. Calibration bar: 50 μm in A1 and A2, 20 μm in B1 and B3, 10 μm in C3.

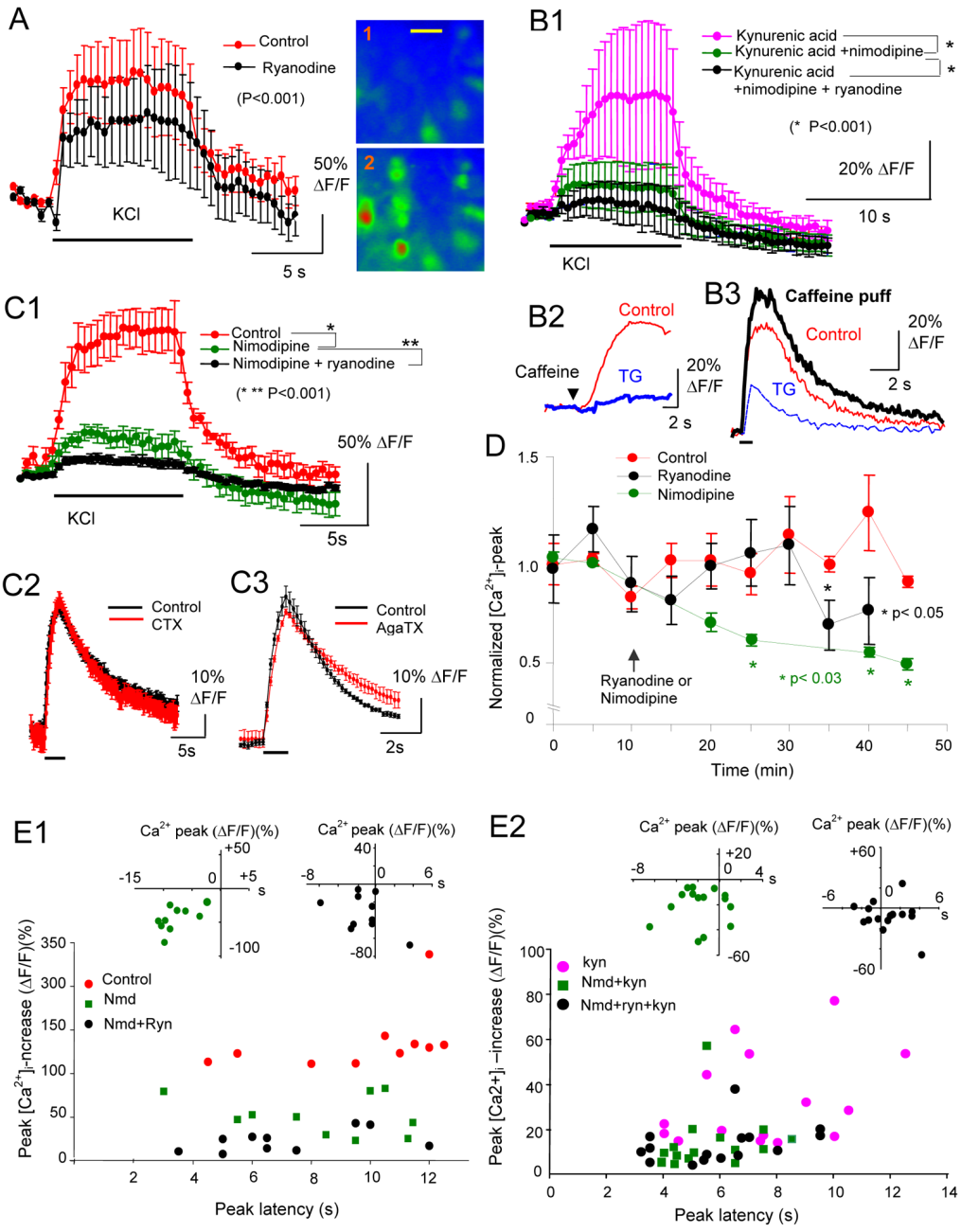

Figure 4.

A. Depolarization-induced $[Ca^{2+}]_i$-elevation and its modulation by ryanodine (traces are shown as mean ± SEM). Inset shows Fluo-3 images before (1) and after (2) KCl puff. Calibration bar: 15 μm. **B1**. Depolarization-induced $[Ca^{2+}]_i$-elevation in the presence of kynurenic acid, nimodipine, and ryanodine. **B2**. Responses to caffeine in the control ACSF and the thapsigargin (TG)-containing ACSF in neurons. **B3**. The same neurons in B2 generated a $[Ca^{2+}]_i$-increase in response to KCl-induced depolarization. A caffeine-puff of 5s immediately before the depolarization (indicated by a horizontal bar) amplified a peak amplitude of the $[Ca^{2+}]_i$-increase. On the other hand, TG reduced the $[Ca^{2+}]_i$-peak to less than 1/3 of the control. **C1**. Depolarization-induced $[Ca^{2+}]_i$-elevation in the control ACSF and its reduction by nimodipine

and ryanodine. **C2**. Effect of ω-conotoxin on depolarization-induced $[Ca^{2+}]_i$-elevation. **C3**. Effect of ω-agatoxin on depolarization-induced $[Ca^{2+}]_i$-elevation. **D**. Time-dependent changes in depolarization-induced $[Ca^{2+}]_i$-elevation in control, nimodipine, and ryanodine. **E1**. Changes in peak amplitude and peak latency of depolarization-induced $[Ca^{2+}]_i$-elevation by ryanodine and nimodipine. Inset shows differences in peak $[Ca^{2+}]_i$-elevation and the peak latency between control and nimodipine (green) and between nimodipine and nimodipine plus ryanodine (black). **E2**. Changes in the identical parameters shown in E1 in the presence of kynurenic acid in ACSF.